EPJ Nuclear Sci. Technol. **11**, 8 (2025)

https://doi.org/10.1051/epjn/2025002

EPJ Nuclear Sciences & Technologies

Available online at:
https://www.epj-n.org

**Status and advances of Monte Carlo codes for particle transport simulation, edited by Andrea Zoia, Cheikh Diop and Cyrille de Saint Jean**

REGULAR ARTICLE

OPEN ACCESS

# Capability overview of the DIANE multiparticle transport code

Benoit Avez*, Eric Brière de l'Isle, Bertrand Cochet, Johan Durand, Frédéric Fernex, Brunella Martin, Amine Nasri and Amaury Walbron

CEA, DAM, CEA-DIF, Bruyères-le-Châtel, F-91297 Arpajon, France

Received: 11 October 2024 / Received in final form: 20 December 2024 / Accepted: 30 January 2025

**Abstract.** The DIANE code is a simulation software that solves the transport equation for neutrons, photons, electrons and light ions using the Monte Carlo method. The DIANE code can perform various kinds of calculations, such as criticality or shielding simulations. This paper presents an overview of the DIANE code capabilities, going through the description of input data, the transport simulation and some examples of applications.

## 1 Introduction

Result of over 40 years of developments, the DIANE code [1] is the reference stochastic particle transport code for CEA DAM at Bruyères-le-Châtel. From its inception, DIANE has been built and maintened with the aim of including physical models at their state of art (in terms of completeness, precision and performance). The result is a code that is capable of conducting coupled neutron-photon-electron and light charged particle Monte Carlo transport, on a fixed and/or evolving geometry such as an Inertial-Confinement-Fusion plasma target.

As other Monte-Carlo codes like MCNP [2] or TRIPOLI-4® [3], the DIANE code can perform various kinds of calculations, such as criticality or shielding simulations. Moreover, it can also be used to study Inertial-Confinement fusion which is one of the various nuclear technologies studied to produce sustainable energy according to electric energy demands in the world. In the present work, we describe main features associated with DIANE and illustrate them through several examples.

## 2 General features for Monte-Carlo particle transport simulations with DIANE

Based on a multi-group formalism, DIANE is used to compute a series of tallies for neutrons, photons, electrons and light ions. Calculations can be performed on one, two or three dimensional geometries, which are described with specific DIANE input cards, but it is also possible to do so by MCNP cards thanks to a geometry converter. A third available approach consists of a mix of both geometries as input. DIANE input cards allow for the description of fixed or evolving geometries with Euler or Lagrange mesh grids. The mesh grid can contain up to millions of cells and the calculations can follow the evolution of a geometry through thousands of time steps. This is particularly useful for example to describe the particle transport physics for an imploding capsule used in experiments led in large ignition facilities such as the NIF in Lawrence Livermore National Laboratory (California, USA) or the Laser Mégajoule in France.

Monte-Carlo particle transport involves tracking the lives of a large number of similar particles, and the simulation for each particle – or batch of particles – can be done in parallel to increase computational efficiency. DIANE performs its calculations in a massively parallel context through MPI instructions [4] so far. However, since studied configurations require an increasing memory consumption (for instance, because of the geometry modelling), recent work has been made to implement a hybrid parallel programming model using the OpenMP library [5] for multi-threading purpose. Yet sometimes, having a large number of parallel processes is not enough to achieve convergence for Monte-Carlo calculations and specific variance reduction techniques have been added in the code over the years.

## 3 Monte-Carlo techniques used in DIANE

Solving the Boltzmann equation (with or without Fokker-Planck terms [6]) through the simulation of stochastic processes can mainly be done in forward or adjoint transport calculations. In both cases, computation time can be prohibitive in the case of complex geometries without variance reduction strategies. The DIANE code can perform particle transport calculations in both forward and adjoint ways, and variance reduction techniques such as weight-window [7,8] and $\delta$-tracking [9] has been implemented to

* e-mail: benoit.avez@cea.fr

be as automated as possible. In order to get access to physical observables, a range of tallies are available such as:

- effective multiplication coefficient $K_{\text{eff}}$;
- point detector;
- surface tallies like currents;
- volume tallies such as energy deposition, fluxes and reaction rates;
- radiograph and pinhole image tallies.

Diagnostic and radiation shielding simulations usually consist of transporting particles emitted from a source through a medium until it reaches a detector. By geometric construction, such calculations are very time consuming without variance reduction methods and thus, they make good examples of how Monte-Carlo techniques can be used in the code: in a first step, DIANE performs an adjoint calculation, which result is then used in a forward more precise calculation to obtain convergence with a significant gain in computation efficiency. Moreover, the simulation of diagnostics requires an accurate description of the detector's response and DIANE is capable of taking it into account.

## 4 Nuclear data

Particle transport codes have two approaches regarding how they use nuclear data: the first one consists of using the continuous representation and therefore make no approximation on data treatment, at the cost of a high computation time and an important memory consumption. The other approach is based on the multigroup approximation in which nuclear data are given on an energy and angular grid. Using this approximation requires specific techniques to account for self-shielding and resonances in general, but also allows for a significant gain in calculation speed and memory cost. Multigroup data are provided by the nuclear data code ZADIG which is developed in CEA DAM. ZADIG groups cross sections from international data libraries in ENDF-6 format according to the multigroup bin structure. It puts the data into the transport multigroup bin structure (energy binning, equiprobable or equi-cosinus angular bin boundaries). To better account for resonances, a specific multigroup treatment option has been implemented in DIANE, called minigroup method. Nuclear data libraries can be specified differently for each particle type and material. Furthermore, the thermalization can be dealt with either ZADIG by including it in the cross sections or by DIANE through a fictitious scattering method [10].

## 5 Applications

DIANE simulates the transport of particles through media, an area of science that is closely related to a large variety of physics. In the present section, we describe through several examples how DIANE is used to conduct scientific studies and researches in nuclear physics and particle transport modelling.

**Table 1.** Selected benchmarks with their relevant parameters (steel thicknesses and experimental $K_{\text{eff}}$).

| Case | Steel thickness (cm) | $K_{\text{eff}} \pm 3\sigma$ |
|---|---|---|
| Pu-Met-Fast-025.C01 | 1.55 | $1 \pm 0.0060$ |
| Pu-Met-Fast-026.C01 | 11.90 | $1 \pm 0.0072$ |
| Pu-Met-Fast-028.C01 | 19.65 | $1 \pm 0.0066$ |
| Pu-Met-Fast-032.C01 | 4.49 | $1 \pm 0.0060$ |

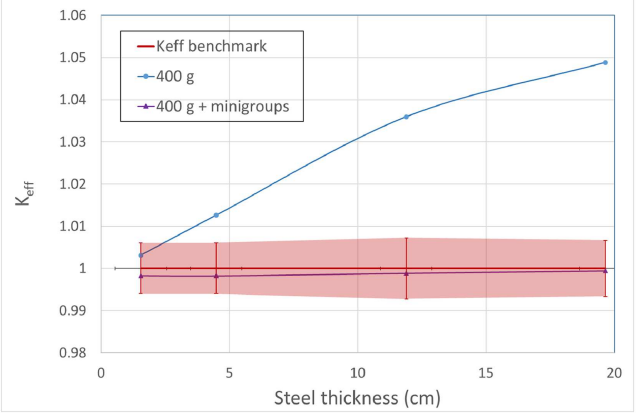


**Fig. 1.** Experimental and simulated $K_{\text{eff}}$ of the four selected benchmarks. Experimental uncertainty corresponds to a confidence level of 99.73% ($3\sigma$). Simulation uncertainty can be neglected (below 5/100000).

### 5.1 Benchmarking multigroup cross-section representations with or without minigroup structure

In order to determine the impact of the use of the minigroup structure on the $K_{\text{eff}}$ calculations, focus is made on steel-reflected configurations, for which high-energy resonances of $^{56}$Fe contained in steel are expected to probe the quality of the groupwise neutron data representations. A set of four benchmarks has been chosen in the ICSBEP dababase [11], all sharing the same geometry: a sphere of metallic plutonium surrounded by a steel reflector. All benchmarks differ with their steel thicknesses, fissile dimensions being adjusted in order to have critical configurations. Main characteristics of the four selected configurations are given in Table 1.

Criticality calculations on these configurations have been performed with the Monte Carlo code DIANE, using (i) a 400-groups mesh and (ii) a 400-groups mesh with minigroup structure, both obtained from the same ENDF/B-VII.1 evaluation [12]. The results are shown in Figure 1. Whereas the use of the 400-groups mesh shows an increasing deviation of calculated $k_{\text{eff}}$ with respect to experimental values as the steel thickness increases, the 400-groups mesh with minigroup structure shows a much better reproduction of experimental values.

### 5.2 Photonuclear reactions

In many cases, nuclear reactions produce high energy gammas and electrons which can themselves interact with nuclei and generate what is called a cascade of reactions. Nuclear reactions induced by a gamma particle are usually named photonuclear reactions and neutrons that are produced from such processes are called photoneutrons. A classical way to study photoneutron production follows a 3-step pattern:

1. high energy electrons are produced with an accelerator;
2. gammas are produced through Bremsstrahlung processes in a thick target with high Z number such as tungsten;
3. high energy gammas interact with a target and produce photoneutrons which are then counted by an appropriate detector.

Simulating this multi-step process requires the computation of the electron-photon cascade, the transport of photons with explicit treatment of photoatomic and photonuclear reactions, and the transport of neutrons. DIANE can perform the coupled neutron-photon transport calculation considering both photoatomic and photonuclear reactions. While the code can simulate a full electron transport, it can also use a processing made by the ZADIG code and based on the Secondary Source Bremsstrahlung (SSB) model [13–15] to compute the electron-photon cascade.

Figure 2 shows the results of a photonuclear benchmark simulation made with DIANE code: a monoenergetic electron beam with 20 MeV of kinetic energy interacts with a 2 mm thick rectangular target made of $^{181}$Ta, located 2 cm away from the source. Photons produced (mostly through Bremsstrahlung processes) can then cause photonuclear reactions in a sphere – 3 cm in radius – of natural uranium placed 4.8 cm away from the $^{181}$Ta target. The spectrum of resulting photoneutrons (including those emitted through photofission processes) is displayed in the aformentioned figure.

Since the early 2000s, a stronger emphasis has been put on studying the Monte-Carlo simulation of photonuclear reactions due to their role in radiation shielding and nuclear instrumentation. The lack of reliable, precise experimental data has led physicists to conduct code-to-code comparisons [16] which show a global agreement between Monte-Carlo codes MCNP6, TRIPOLI-4® and DIANE. However, significant discrepancies appear between the codes and their major source seems to be the electron-photon cascade. Further investigations are on the way [17], involving the production of new experimental data and more comparisons between the previousely mentionned codes and the possible inclusion of PHITS [18] and GEANT4 [19–21] codes.

### 5.3 Transport in stochastic media

The DIANE code is able to perform particle transport in stochastic media, i.e. media in which the material properties at a given point in space are only known statistically

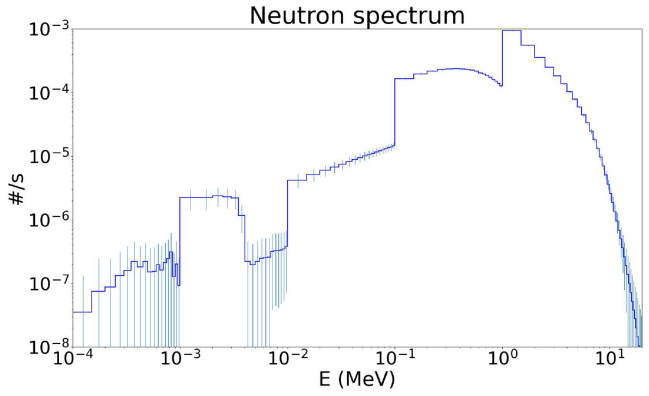


**Fig. 2.** Normalized energy spectrum of photoneutron emitted by the natural uranium target irradiated by the photons produced from Bremsstralhung processes of 20 MeV electrons on the $^{181}$Ta conversion target. Simulation uncertainty corresponds to a confidence level of 95.0% ($2\sigma$).

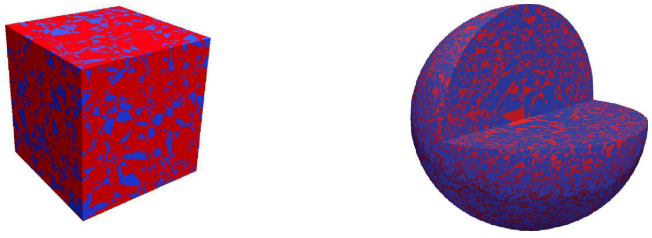

**Fig. 3.** Example of 3D realizations of a spatially homogeneous (left) and a spatially heterogeneous (right) stochastic medium with binary mixture, taken from references [30,32]. Each color refers to a material property assignment in the geometries.

[22–24]. Several applications emerging in nuclear science and engineering require the modeling of particle transport in such disordered media. Examples are widespread and concern for instance the study of the propagation of photons in the hydrodynamical instabilities at the material interfaces in inertial confinement fusion pellets driven by lasers [25,26].

The model implemented in DIANE is the standard form of the famous Chord Length Sampling (CLS) algorithm [26,27] which formally solves the Levermore-Pomraning equations for Markovian binary mixing [28,29]. CLS is a Monte Carlo method based on the sampling "on-the-fly" of pseudo-interfaces between the different material components of the stochastic media during the particles displacements by drawing the distances to the following material boundaries from a distribution depending on the mixing statistics. CLS is an *annealed disorder* approach since the spatial configuration seen by each particle is regenerated at each particle flight. Thus, by construction, spatial correlations are neglected with this effective model because the memory of the crossed material pseudo-interfaces is systematically lost. Consequently, CLS might show discrepancies with respect to reference solutions – obtained via the so-called *quenched disorder* approach at the expense of high computational cost by solving the Boltzmann equation for a

**Table 2.** Analytical and calculated values of $K_{\text{eff}}$ for a subset of benchmarks extracted from [37]. Calculated values are given for both collision and track-length tallies with their statistical uncertainties.

| Benchmark name | $K_{\text{analytical}}$ | $K_{\text{track-length}}$ | $\sigma$ ($10^{-5}$) | $K_{\text{collision}}$ | $\sigma$ ($10^{-5}$) |
|---|---|---|---|---|---|
| Ua-1-0-SL | 2.61290 | 2.61296 | 5 | 2.61293 | 5 |
| UD2O-1-0-SL | 1.00000 | 0.99999 | 2 | 0.99999 | 2 |
| PUa-H2O(1)-1-0-SL | 1.00000 | 0.99998 | 2 | 0.99999 | 2 |
| PU-2-0-IN | 1.00000 | 0.99997 | 2 | 0.99998 | 2 |
| UAL-2-0-SP | 2.29032 | 2.29038 | 5 | 2.29035 | 4 |
| URRd-2-0-IN | 1.00000 | 0.99998 | 2 | 0.99995 | 2 |
| URR-3-0-IN | 1.00000 | 1.00004 | 2 | 1.00001 | 2 |
| PUb-1-0-SP | 1.00000 | 0.99998 | 2 | 1.00000 | 2 |
| PUb-H2O(1)-1-0-CY | 1.00000 | 1.00002 | 2 | 0.99999 | 2 |
| PUb-H2O(10)-1-0-CY | 1.00000 | 1.00001 | 2 | 1.00001 | 2 |
| Ua-1-0-IN | 2.25000 | 2.25002 | 2 | 2.25003 | 2 |
| Ua-1-0-CY | 1.00000 | 1.00002 | 2 | 1.00000 | 2 |
| Ua-1-0-SP | 1.00000 | 0.99999 | 2 | 0.99998 | 2 |
| Ub-1-0-IN | 1.00000 | 0.99996 | 3 | 0.99999 | 2 |
| Ub-H2O(1)-1-0-SP | 2.33092 | 2.33097 | 5 | 2.33094 | 4 |
| Uc-1-0-IN | 1.00000 | 0.99998 | 3 | 0.99997 | 2 |
| Uc-H2O(1)-1-0-SP | 2.25608 | 2.25615 | 3 | 2.25613 | 3 |
| Ud-1-0-IN | 1.00000 | 1.00002 | 2 | 1.00002 | 2 |
| PUa-1-0-IN | 2.23267 | 2.23272 | 3 | 2.23270 | 3 |
| Ud-H2O(1)-1-0-SP | 1.00000 | 0.99998 | 3 | 1.00000 | 2 |

large number of realizations of random media, involving "frozen" spatial configuration for all the traversing particles – but is convenient in practical applications where a trade-off between computational time and precision is mandatory.

DIANE is taking advantage of the significant improvements that has been made in both approaches in the last years, part of them being the results of a fruitful collaboration between CEA/DES and CEA/DAM throughout the projects GEOSTOH (2021) and TRANSPAREMS (2023):

- For the *quenched disorder* approach: a rigourous mathematical framework has been establish and a simulation tool has been developed [30,31] to sample a set of three-dimensional Markovian media with the hypothesis of spatial homogeneity, i.e. the characteristic scale of the disorder being the same at any point in space. The homogeneity assumption has been then relaxed for three-dimensional media [32]. For illustration, an example of realizations of random media is provided in Figure 3. The ability to take into account non-homogeneous statistical properties, and in particular spatial gradients, turns out to be essential in the modeling of realistic disordered structures, such as the stratification of materials due to gravity or the complex interfaces of multiphase mixtures like Rayleigh-Taylor instabilities. Whereas reference results were almost exclusively limited to the dimension 1 for reasons of algorithmic complexity and computational requirements, this major breakthrough has allowed calculating, initially with TRIPOLI-4®, reference solutions in dimension 3 with and without spatial gradients [31,32], which are required to evaluate the predictive power of *annealed disorder* models to real-world configurations. Within recent developments, DIANE is now able to access such results. Their validity has been shown through code-to-code comparison with TRIPOLI-4® and illustrate the good agreement between both codes [33];
- For the *annealed disorder* approach: the comparison between the results obtained by CLS methods on the aforementioned configurations and reference results has revealed discrepancies that can be mainly attributed to the absence of memory in the processing of the effects of disorder [32,34]. Therefore, a generalization of CLS algorithms including partial memory effects due to correlations for particles crossing back and forth between the same materials have been proposed for the three-dimensions homogeneous configurations – including Poisson-Box Sampling (PBS) [35] developed at CEA/DES – and is currently being developed for inhomogeneous cases [36]. The basic idea behind spatial memory effects is that the particles remember the position of the last interfaces crossed, and this during several consecutive movements [35] instead of regenerating the material pseudo-interfaces each time the particles move. By increasing the number of interfaces that each particle remembers, the accuracy of these effective methods with spatial memory increases considerably, at the expense of computation time. These

models are planned to be implemented and tested in DIANE soon.

## 6 Outlooks for DIANE

DIANE is the result of several decades of development and, as for other scientific codes that were written in the eighties, its maintenance and evolution can prove cumbersome. Therefore, an effort is undergoing at CEA DAM to modernize the code with up-to-date programming and computing techniques, including:

- A modern component-oriented core that carries complex data structure and algorithms;
- A user interface with bindings to the core;
- A hybrid parallel programming model;
- The use of software quality tools for testing, version control and continuous integration.

Aside from various unitary and integration tests, the code is continuously verified using code-to-code comparisons and with analytical benchmarks. In particular, the criticality algorithm is verified against analytical benchmarks extracted from [37]. Results obtained on a subset of these benchmarks are summarized in Table 2 for $K_{\text{eff}}$ values obtained from both collision and track-length tallies, with good agreement between calculated and analytical values.

Finally, we are also considering the extension of current capabilities of DIANE, including portability on GPU supercomputers. Regarding performance improvements, we are also searching for models dealing with Woodcock algorithm to see if a reliable method leading to sizeable better computation time can be found.

### Funding

This research did not receive any specific external funding.

### Conflicts of interest

The authors declare that they have no competing interests to report.

### Data availability statement

Data associated with this article cannot be disclosed.

### Author contribution statement

All authors have contributed to this work, to the computations and to the analyses.

### References

1. M. Caillaud, S. Lemaire, S. Ménard, P. Rathouit, J.C. Ribes, D. Riz, SNA + MC 2013 – Joint International Conference on Supercomputing in Nuclear Applications + Monte Carlo (2014)
2. MCNP Code Version 6.3.0 Theory & User Manual, Los Alamos National Laboratory, LA-UR-22-30006, Rev. 1 (2022)
3. E. Brun, F. Damian, C. Diop, E. Dumonteil, F. Hugot, C. Jouanne, et al., TRIPOLI-4, CEA, EDF and AREVA reference monte carlo code, Ann. Nucl. Energy **82**, 151 (2015)
4. A Message-Passing Interface Standard Version 4.0 (2021), https://www.mpi-forum.org/docs/mpi-4.0/mpi40-report.pdf
5. L. Dagum, R. Menon, OpenMP: an industry standard API for shared-memory programming, IEEE Comput. Sci. Eng. **5**, 46 (1998)
6. B.P. Nigam, et al., Phys. Rev. **115**, 491 (1959)
7. W.L. Thompson, O.L. Deutsch, T.E. Booth, Deep-Penetration Calculations, A Review of the Theory and Application of Monte Carlo Methods, in *Proceedings of a Seminar-Workshop, Oak Ridge Tennessee, April 21–23, ORNL/RSIC-44* (1980)
8. W.L. Thompson, E.D. Cashwell, The Status of Monte Carlo at Los Alamos, A Review of the Theory and Application of Monte Carlo Methods, in *Proceedings of a Seminar-Workshop, Oak Ridge Tennessee, April 21–23, ORNL/RSIC-44* (1980)
9. E. Woodcock, T. Murphy, P. Hemmings, S. Longworth, Techniques used in the GEM code for Monte Carlo neutronics calculations in reactors and other systems of complex geometry, in *Proc. Conf. Application of Computing Methods to Reactor Problems, ANL-7050, Argone National Laboratory* (1965)
10. L.L. Carter, E.D. Cashwell, W.M. Tatlor, Nucl. Sci. Eng. **48**, 403 (1972)
11. International Handbook of Evaluated Criticality Safety Benchmark Experiments 2021, Vol. I, NEA/NSC/DOC(95)03
12. M.B. Chadwick, et al., ENDF/B-VII.1 Nuclear Data for Science and Technology: Cross Sections, Covariances, Fission Product Yields and Decay Data, Nucl. Data Sheets **112**, 2887 (2011)
13. S. Kitsos, et al., Nucl. Sci. Eng., **123**, 215 (1996)
14. D. Riz, M. Caillaud, Proc. ANS Physor, Pittsburgh, USA (2000)
15. C. Toccoli, et al., Nucl. Technology, **168**, 933 (2009)
16. T.K. Tuyet, et al., ICRS14/RPSD (2022)
17. A. Sari, et al. (to be published)
18. T. Sato, et al., Recent improvements of the Particle and Heavy Ion Transport code System – PHITS version 3.33, J. Nucl. Sci. Technol. **61**, 127 (2024)
19. S. Agostinelli, et al., Nucl. Instrum. Meth. A **506**, 250 (2003)
20. J. Allison, et al., IEEE Trans. Nucl. Sci. **53**, 270 (2006)
21. J. Allison, et al., Nucl. Instrum. Meth. A **835**, 186 (2016)
22. G.C. Pomraning, *Linear Kinetic Theory and Particle Transport in Stochastic Mixtures* (World Scientific Publishing, NJ, USA, 1991)
23. G.C. Pomraning, Adv. Nuc. Sci. Tech. **24**, 47 (1996)
24. S. Torquato, *Random Heterogeneous Materials: Microstructure and Macroscopic Properties* (Springer-Verlag, New York, USA, 2013)
25. O. Haran, D. Shvarts, R., Thieberger, Phys. Rev. E **61**, 6183 (2000)
26. G.B. Zimmerman, Lawrence Livermore National Laboratory Report UCRL-JC-105616 (1990)
27. G.B. Zimmerman, M.L. Adams, Trans. Am. Nucl. Soc. **66**, 287 (1991)
28. D.C. Sahni, J. Math. Phys. **30**, 1554 (1989)
29. D.C. Sahni, Ann. Nucl. Energy **16**, 397 (1989)
30. C. Larmier, Stochastic Particle Transport in Disordered Media: Beyond the Boltzmann Equation, Université Paris-Saclay, France (2018)

31. C. Larmier, F.-X. Hugot, F. Malvagi, A. Mazzolo, A. Zoia, Benchmark solutions for d-dimensional Markov binary mixtures, J. Quant. Spectrosc. Radiat. Transf. **189**, 133 (2017)
32. M.A. Kowalski, C. Larmier, F. Madiot, J. Durand, S. Lemaire, A. Zoia, Particle transport in Markov media with spatial gradients: Comparison between reference solutions and Chord Length Sampling, J. Quant. Spectrosc. Radiat. Transf. **286**, 108185 (2022)
33. Internal report CEA/DAM
34. C. Larmier, A. Lam, P. Brantley, F. Malvagi, T. Palmer, A. Zoia, Monte Carlo Chord Length Sampling for d-dimensional Markov binary mixtures, J. Quant. Spectrosc. Radiat. Transf. **204**, 256 (2018)
35. C. Larmier, A. Zoia, F. Malvagi, E. Dumonteil, A. Mazzolo, Poisson-Box Sampling algorithm for three-dimensional Markov binary mixtures, J. Quant. Spectrosc. Radiat. Transf. **206**, 70 (2018)
36. A. Tentori, C. Larmier, J. Durand, B. Cochet, A. Zoia, Phys. Rev. E **109**, 035302 (2024)
37. A. Sood, R.A. Forster, D.K. Parsons, Analytical Benchmark Test Set for Criticality Code Verification, LA-UR-01-3082 (2001)

**Cite this article as:** Benoît Avez, Eric Brière de l'Isle, Bertrand Cochet, Johan Durand, Frédéric Fernex, Brunella Martin, Amine Nasri, Amaury Walbron. Capability overview of the DIANE multiparticle transport code, EPJ Nuclear Sci. Technol. **11**, 8 (2025). https://doi.org/10.1051/epjn/2025002.